Testing Higher-Order Quantum Interference with Many-Particle States

Marc-Oliver Pleinert[1,2] Alfredo Rueda,[1,*] Eric Lutz,[3] and Joachim von Zanthier[1,2]

[1]*Institut für Optik, Information und Photonik,*
Friedrich-Alexander-Universität Erlangen-Nürnberg (FAU), 91058 Erlangen, Germany
[2]*Erlangen Graduate School in Advanced Optical Technologies (SAOT),*
Friedrich-Alexander-Universität Erlangen-Nürnberg (FAU), 91052 Erlangen, Germany
[3]*Institute for Theoretical Physics I, University of Stuttgart, D-70550 Stuttgart, Germany*

Quantum theory permits interference between indistinguishable paths but, at the same time, restricts its order. Single-particle interference, for instance, is limited to the second order, that is, to pairs of single-particle paths. To date, all experimental efforts to search for higher-order interferences beyond those compatible with quantum mechanics have been based on such single-particle schemes. However, quantum physics is not bound to single-particle interference. We here experimentally study many-particle higher-order interference using a two-photon-five-slit setup. We observe nonzero two-particle interference up to fourth order, corresponding to the interference of two distinct two-particle paths. We further show that fifth-order interference is restricted to 10^{-3} in the intensity-correlation regime and to 10^{-2} in the photon-correlation regime, thus providing novel bounds on higher-order quantum interference.

Interference phenomena for both light and matter are an intrinsic property of quantum physics. They occur when indistinguishable paths exist, as in Young's paradigmatic double-slit experiment [1]. From a fundamental point of view, quantum interference stems from coherent superpositions of states and thus from the linearity of quantum theory [2]. However, quantum mechanics not only enables but also restricts interference [3]. For instance, according to Born's rule, which relates detection probabilities to the modulus square of the wave function [4], single-particle interference is limited to the second order, that is, to two interfering single-particle paths. In a multislit setup, interference is therefore expected to occur only between pairs of indistinguishable paths, and all higher orders in the interference hierarchy vanish [3].

The physical origin of the lack of higher-order quantum interferences is not yet understood [3]. Their existence would have profound implications for quantum theory, including nonlocality and contextuality [5–8]. They have indeed been linked to violations of the spatial [5] and temporal [6] Tsirelson bounds, as well as to a weakening of noncontextuality bounds [7]. They would hence reveal entanglement stronger than predicted by quantum theory. They would further permit perfect interaction-free measurements [8]. For this reason, a growing number of single-particle experiments have been realized in the past years to detect such higher-order interference, using photons in the optical [9–12] and microwave [13] domain, as well as molecules [14], atoms [15], and spin systems [16,17]. However, while high-sensitivity tests of the linearity of quantum mechanics have been performed [18–24], similar experiments on higher-order interference are missing.

Quantum physics goes beyond single-particle interference by allowing for many-particle interference in the case of indistinguishable particles. A prominent example is provided by the Hong-Ou-Mandel experiment, in which two noninteracting photons can influence each other via two-particle interference [25]. Many-particle interference, described by Glauber's theory of quantum optical coherence [26], is mathematically richer and physically more subtle than single-particle interference [27–30]. It has found widespread applications in metrology [31,32], imaging [33–35], and quantum information processing [36,37]. Recently, the interference hierarchy has been theoretically extended to the general case of M-particle interference with N modes [38]. In this situation, Born's rule allows for higher-order path interference of up to order $2M$. In addition, owing to the much larger number of interfering paths, many-particle interference has been predicted to offer increased sensitivity to deviations from quantum theory compared to its single-particle counterpart [38].

We here report the first experimental investigation of many-particle higher-order quantum interference using a two-photon-five-slit setup. We determine single-particle and two-particle interferences up to fifth order, both in the intensity and in the photon-counting regimes. To this end, we measure and evaluate first-order and second-order (spatial) correlation functions for a total of $2^5 = 32$ different interference configurations. While single-particle interference vanishes at the third order, we show that two-
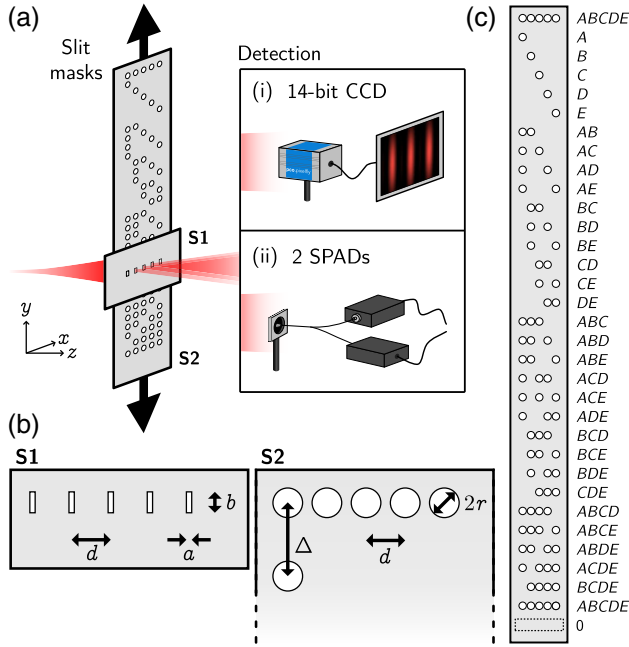
FIG. 1. (a) Setup to measure the interference hierarchy in single-particle and two-particle interferences. Coherent photons are sent through two slit masks, S1 and S2, and measured in the far field, either (i) by a charge coupled device (CCD) or (ii) by two single photon avalanche diodes (SPADs). (b) Fixed base slit mask S1 with dimensions $a = 25 \, \mu m$, $b = 200 \, \mu m$, and $d = 500 \, \mu m$. The dimensions of the movable slit mask S2 are $2r = 400 \, \mu m$ with a spacing $\Delta = 1000 \, \mu m$. (c) The layout of slit mask S2 contains 33 configurations.

particle interference only cancels at the fifth order, in agreement with standard quantum theory.

Experimental setup.—In order to assess single-particle and two-particle interference orders, we realize and analyze different experimental arrangements [Fig. 1(a)]: Photons, in a coherent state $|\alpha\rangle$ with mean photon number $\bar{n} = |\alpha|^2$, are provided by a HeNe laser at $\lambda = 633$ nm. These photons are scattered at two slit masks S1 and S2 [Figs. 1(b) and 1(c)]. The base slit mask S1 is a five-fold slit (denoted *ABCDE*), while the movable blocking slit mask S2 consists of 33 configurations. Both masks have the same distance of adjacent slits $d = 500 \, \mu m$. By moving the blocking slit mask S2 in front of the fixed slit mask S1, we can implement all possible slit arrangements from one to five slits. For instance, in Fig. 1(a), slits A and E of S1 are blocked by S2 such that the three-slit configuration BCD is realized. The measurement is conducted in the far field at a distance $L = 1.7$ m behind the first slit mask, in either (i) the intensity regime by a specialized, high-performance 14-bit charge-coupled device (CCD) camera or (ii) the photon-counting regime by two fiber-coupled single photon avalanche diodes (SPADs) whose signals are time-registered and correlated [39]. In this far-field regime, effects coming from nonclassical looped paths [40–42] are negligible [38].

During a measurement sequence, the source, the base mask S1, and the detection systems are fixed, while the blocking mask S2 is scanned in a fully automatized way to reduce alignment errors [39]. Data acquisition is also fully automatized. A second five-fold slit *ABCDE* has moreover been added at the top of S2 to compare the interference patterns at the beginning and the end of mask S2 and thus verify the initial alignment of the setup [39].

The measurement results can be interpreted in the few-particle regime by expanding the coherent state as

$$|\alpha\rangle = c_0|0\rangle + c_1|1\rangle + c_2|2\rangle + \ldots, \quad (1)$$

where $p_n = |c_n|^2$, $(n = 0, 1, 2, \ldots)$, is the Poissonian probability of the n-photon state to occur. Whenever we register a photon at only one of the two SPADs, the effective state is given by $|1\rangle$, which has been coherently distributed over the slits, leading to single-particle interference. For a coincident detection at both detectors, the effective state is $|2\rangle$, yielding two-particle interference. Accordingly, we can measure both interference hierarchies simultaneously and differentiate between them by filtering the events via postselection [43].

Interference hierarchy.—Although they are noninteracting, identical photons can influence each other via interference of distinct but indistinguishable M-particle paths. Such M-particle paths lead to (spatial) correlations between field modes that can be conveniently captured, on the photon as well as on the intensity level, by the Mth-order correlation function [26],

$$G^{(M)}(\delta_1, \ldots, \delta_M) \propto \langle \hat{a}_1^\dagger \ldots \hat{a}_M^\dagger \hat{a}_M \ldots \hat{a}_1 \rangle, \quad (2)$$

where $\hat{a}_i \equiv \hat{a}(\delta_i)$ is the annihilation operator of the spatial mode $\delta_i = kd \sin\theta_i$, determined by the wave vector k, the slit distance d, and the angle of the ith detector θ_i. Interference in such M-particle correlations can be classified into various orders $I_N^{(M)}$, depending on how many different input modes (A, B, …) interfere with each other.

For single particles ($M = 1$), the first-order interference is trivially given by the (relative) detection probability in the far field, $I_1^{(1)} = P_A = G_A^{(1)}$, for a single slit A. The second-order interference is obtained by comparing the quantum-mechanical double-slit (AB) signal with the classical sum of the two single slits (A and B) [3],

$$I_2^{(1)} = G_{AB}^{(1)} - [G_A^{(1)} + G_B^{(1)}]. \quad (3)$$

Higher orders can be constructed accordingly [3,38], and the explicit expressions are given in Fig. 2. For single-particle correlations, all higher-order terms vanish, $I_3^{(1)} = I_4^{(1)} = I_5^{(1)} = \ldots = 0$ [3]. The single-particle interference hierarchy hence truncates at the third order.
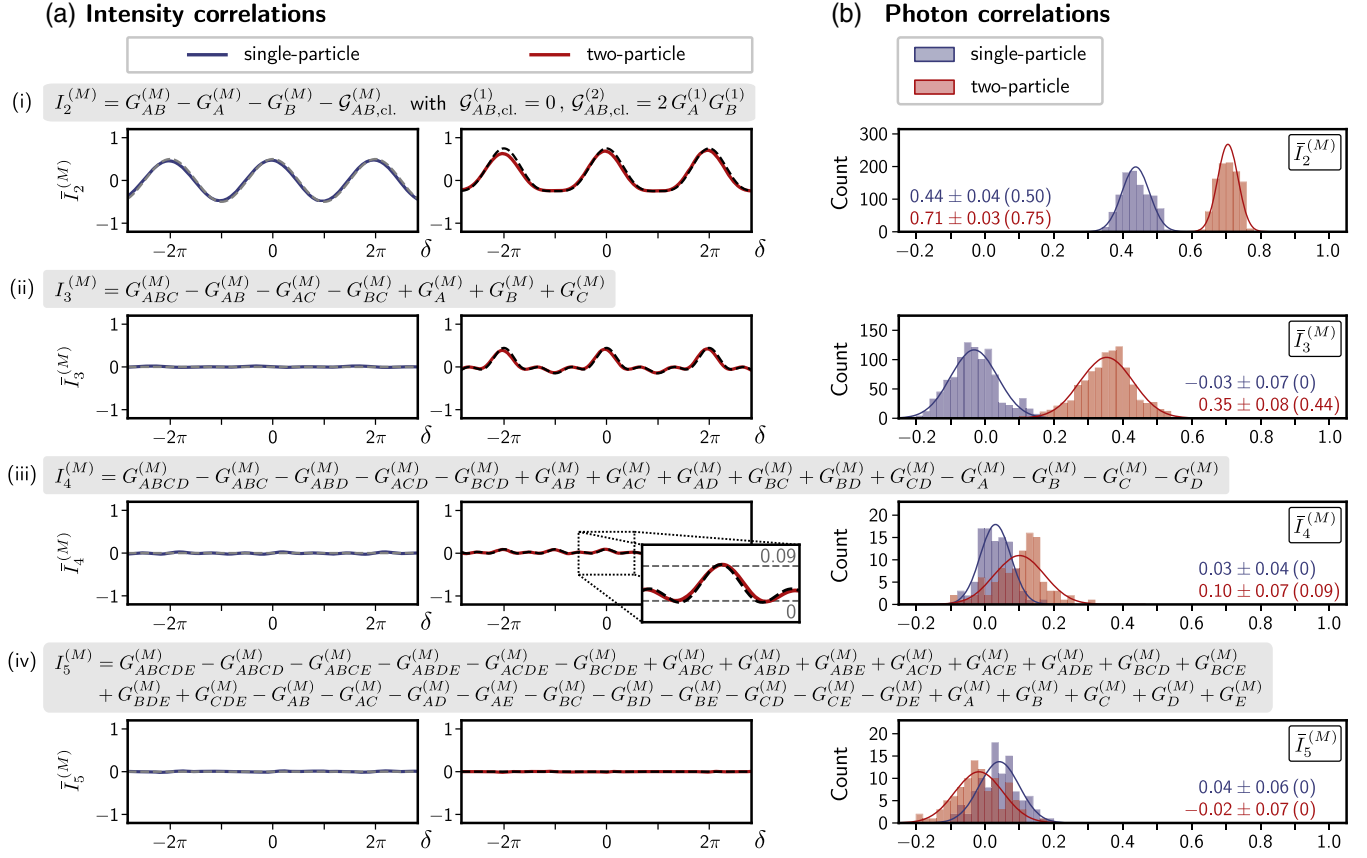
FIG. 2. Interference hierarchy in (a) the intensity-correlation and (b) the photon-correlation regime from (i) second order to (iv) fifth order (related formulas are taken from Ref. [38]). (a) Experimental data (solid) and quantum theory (dashed) of single-particle (blue, left) and two-particle (red, right) interference orders. Fourth-order two-particle interference exhibits a tiny modulation, clearly visible with a good signal-to-noise ratio and most pronounced at the center (inset). (b) Histograms of the single-particle (blue) and two-particle (red) interference hierarchy at $\delta = 0$ in the photon-counting regime.

By contrast, for two particles ($M = 2$), nonzero interference occurs up to the fourth order [38],

$$I_2^{(2)} \neq 0, I_3^{(2)} \neq 0, I_4^{(2)} \neq 0; \qquad I_5^{(2)} = I_6^{(2)} = \ldots = 0. \quad (4)$$

Born's rule hence allows for the interference of two two-particle paths, and the two-particle interference hierarchy is only truncated at the fifth order [44].

The vanishing of many-particle higher-order interference is captured by the M-particle Sorkin parameter defined as the normalized $(2M + 1)$th interference order [38],

$$\kappa^{(M)} = \frac{I_{2M+1}^{(M)}}{G_{A,B,C,\ldots}^{(M)}(0, 0, 0, \ldots)}, \quad (5)$$

where the first member ($M = 1$) is the single-particle Sorkin parameter [3]. According to quantum mechanics, Eq. (5) is zero for all M.

Experimental results.—To obtain the complete interference hierarchy of single-particle and two-particle correlations, we perform $31 + 1 + 1$ (correlation) measurements.

The latter consist of the measurement of 31 different slit configurations needed to evaluate the interference orders, one additional measurement for the second $ABCDE$ arrangement added at the top of the slit mask S2, and one final measurement of the background (0), where the mask S2 blocks all slits of the base mask S1. These 33 measurements form a measurement set.

At the beginning of such a set, the measurement sequence is randomized to reduce systematic errors. A motorized translation stage addresses the slit mask S2 and implements the drawn slit configuration $X \in \{ABCDE(1), A, B, \ldots, ABCDE(2), 0\}$. In the intensity regime, we take 250 CCD images of each slit configuration. The integration time $t_i = 2$ ms is fixed for all configurations and fully covers the CCD's dynamical range when measuring $ABCDE$. In the photon-counting regime, the two SPADs register the single-photon and two-photon events within a fixed total time of $T = 120$ s per slit configuration. Time tags of the photon events are registered by a time-to-digital converter and correlated within a time frame of $t_f = 1$ ns. We ensure that the count rates are $\lesssim 100$ kHz such that detector nonlinearities can be

neglected [39]. We record the data in the autocorrelation scheme, where both detectors are effectively at the same position ($\delta_1 = \delta_2 = \delta$). This scheme is least sensitive to alignment errors. For intensity measurements, each pixel of the CCD can be regarded as an independent detector, and the autocorrelation function is measured by correlating pixels of the same optical phase δ from neighboring lines of the CCD [39]. On the other hand, for photon-counting measurements, the autocorrelation is implemented by a fiber beam splitter at δ, connected to the two different SPADs.

In total, we perform 100 such measurement sets, each with a different sequence, in the intensity regime as well as in the photon-counting regime. For each set, the data is averaged per slit configuration and corrected by subtracting background and detector noise. From the corrected data, we evaluate the two-particle interference orders $I_2^{(2)}, I_3^{(2)}, I_4^{(2)}, I_5^{(2)}$, as well as the single-particle interference orders $I_2^{(1)}, I_3^{(1)}, I_4^{(1)}, I_5^{(1)}$, from (a subset of) the data as indicated in Fig. 2. We normalize the interference orders by the central value of the configuration with the most slits within a given order to remove any experiment-specific proportionality factors [14,15,42]. For example, for two slits A and B, we use $\bar{I}_{2,AB}^{(2)} = I_{2,AB}^{(2)}/G_{AB}^{(2)}(0,0)$, where we have explicitly indicated the involved slits. For the fifth order in two-particle correlations, this corresponds to the normalized two-particle Sorkin parameter of Eq. (5), $\kappa^{(2)} \equiv \bar{I}_5^{(2)}$.

In the intensity regime, the CCD covers the interval $\delta \in [-3\pi, +3\pi]$ of the interference pattern and thus reveals the spatial behavior of the interference orders. The results for single-particle and two-particle correlations are shown in Fig. 2(a): Solid lines correspond to experimental data and dashed lines to quantum theory. Single-particle interference (blue, left) vanishes starting with the third order, $\bar{I}_N^{(1)} = 0$ for $N \geq 3$, with an uncertainty of 10^{-3}, essentially limited by the relative misalignment of the slit configurations. By contrast, two-particle interference $\bar{I}_N^{(2)}$ (red, right) also exhibits a nonzero third and fourth order, while only the fifth order disappears. The modulation of the fourth-order two-particle interference [inset of Fig. 2(a)] is of the order of 10^{-1}, clearly identifiable with a good signal-to-noise ratio.

The difference between single-particle and two-particle correlations can be seen most prominently at $\delta = 0$, also in the photon-counting regime [Fig. 2(b)]. While single-particle and two-particle correlations exhibit both nonzero interference of the second order (though with a different value due to the normalization), the difference between the two is clearly visible for the third-order term with $\bar{I}_3^{(1)} = -0.03 \pm 0.07$ being effectively zero and $\bar{I}_3^{(2)} = 0.35 \pm 0.08$ being statistically different from zero [45]. The same holds true for the interference of the fourth order with
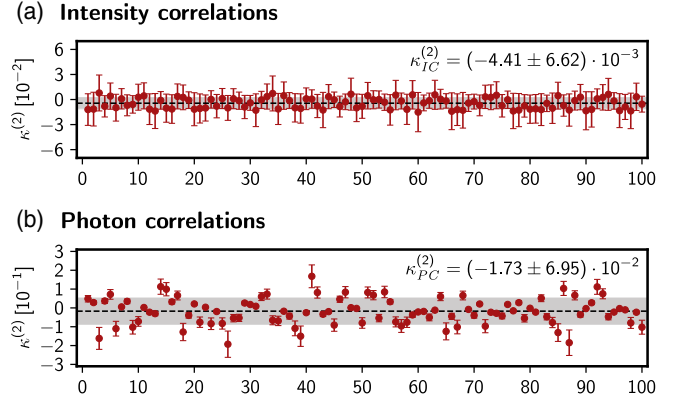

FIG. 3. Two-particle Sorkin parameter $\kappa^{(2)}$ from Eq. (5) for 100 measurement sets in (a) the intensity-correlation regime and (b) the photon-correlation regime. In (b), the error bars are enlarged by a factor of 100.

$\bar{I}_4^{(1)} = 0.03 \pm 0.04$ and $\bar{I}_4^{(2)} = 0.10 \pm 0.07$ [46]. On the other hand, the fifth-order interference is effectively zero for both single-particle and two-particle correlations.

The fifth-order term $\bar{I}_5^{(2)}$ can be used to rule out higher-order interference in two-particle correlations via the Sorkin parameter of Eq. (5). The experimental findings for $\kappa^{(2)}$ are shown in Fig. 3 for (a) intensity correlations (with statistical errors resulting from averaging over different pixels) and (b) photon correlations (with Poissonian errors), each consisting of 100 independent sets of measurements. We obtain $\kappa_{IC}^{(2)} = (-4.41 \pm 6.62) \times 10^{-3}$ in the intensity-correlation (IC) regime and $\kappa_{PC}^{(2)} = (-1.73 \pm 6.95) \times 10^{-2}$ in the photon-correlation (PC) regime.

Conclusions.—We have performed a detailed experimental study of many-particle higher-order interference using a two-photon-five-slit setup, both in the intensity and in the photon-counting regimes. We have observed for the first time fourth-order two-particle interference, corresponding to the interference of two different two-particle paths employing four distinct modes [44]. We have, moreover, established the absence of the corresponding fifth-order interference at the level of 10^{-2}–10^{-3}. The precision of our experiment may be improved further by reducing measurement errors using, for instance, a more stable integrated photonic network scheme with lower losses compared to our free-space setup [47]. The present two-particle interference scheme leads to a tenfold increase in sensitivity [48] to deviations from quantum theory compared to existing single-particle experiments [38]. Because of the exponential increase of interfering paths with growing particle number, this sensitivity is expected to increase significantly: from 1 order of magnitude for the considered two-particle example up to 12 orders of magnitude for eight-particle interference [38]. Since eight-particle experiments have already been realized [49], many-particle interference appears to be a promising

approach for high-sensitivity tests of higher-order quantum interference. An extension toward continuous variables might also be worthwhile for future investigations [50–52].

[*]Present address: Scantinel Photonics, Carl-Zeiss-Strasse 22, 73447 Oberkochen, Germany.

[1] R. Feynman, R. Leighton, and M. Sands, *The Feynman Lectures on Physics* (Addison-Wesley, Reading, 1965).

[2] A. Peres, *Quantum Theory: Concepts and Methods* (Kluwer Academic Publishers, New York, 2002).

[3] R. D. Sorkin, Quantum mechanics as quantum measure theory, Mod. Phys. Lett. A **09**, 3119 (1994).

[4] M. Born, Zur Quantenmechanik der Stoßvorgänge, Z. Phys. **37**, 863 (1926).

[5] G. Niestegge, Three-slit experiments and quantum non-locality, Found. Phys. **43**, 805 (2013).

[6] B. Dakić, T. Paterek, and Č. Brukner, Density cubes and higher-order interference theories, New J. Phys. **16**, 023028 (2014).

[7] J. Henson, Bounding Quantum Contextuality with Lack of Third-Order Interference, Phys. Rev. Lett. **114**, 220403 (2015).

[8] Z. Zhao, S. Mondal, M. Markiewicz, A. Rutkowski, B. Dakić, W. Laskowski, and T. Paterek, Paradoxical consequences of multipath coherence: Perfect interaction-free measurements, Phys. Rev. A **98**, 022108 (2018).

[9] U. Sinha, C. Couteau, T. Jennewein, R. Laflamme, and G. Weihs, Ruling out multi-order interference in quantum mechanics, Science **329**, 418 (2010).

[10] J. M. Hickmann, E. J. S. Fonseca, and A. J. Jesus-Silva, Born's rule and the interference of photons with orbital angular momentum by a triangular slit, Europhys. Lett. **96**, 64006 (2011).

[11] I. Söllner, B. Gschösser, P. Mai, B. Pressl, Z. Vörös, and G. Weihs, Testing Born's rule in quantum mechanics for three mutually exclusive events, Found. Phys. **42**, 742 (2012).

[12] T. Kauten, R. Keil, T. Kaufmann, B. Pressl, Č. Brukner, and G. Weihs, Obtaining tight bounds on higher-order interferences with a 5-path interferometer, New J. Phys. **19**, 033017 (2017).

[13] G. Rengaraj, U. Prathwiraj, S. N. Sahoo, R. Somashekhar, and U. Sinha, Measuring the deviation from the super-position principle in interference experiments, New J. Phys. **20**, 063049 (2018).

[14] J. P. Cotter, C. Brand, C. Knobloch, Y. Lilach, O. Cheshnovsky, and M. Arndt, In search of multipath inter-ference using large molecules, Sci. Adv. **3**, e1602478 (2017).

[15] A. R. Barnea, O. Cheshnovsky, and U. Even, Matter-wave diffraction approaching limits predicted by feynman path integrals for multipath interference, Phys. Rev. A **97**, 023601 (2018).

[16] D. K. Park, O. Moussa, and R. Laflamme, Three path interference using nuclear magnetic resonance: A test of the consistency of Born's rule, New J. Phys. **14**, 113025 (2012).

[17] F. Jin, Y. Liu, J. Geng, P. Huang, W. Ma, M. Shi, C.-K. Duan, F. Shi, X. Rong, and J. Du, Experimental test of Born's rule by inspecting third-order quantum interference on a single spin in solids, Phys. Rev. A **95**, 012107 (2017).

[18] C. G. Shull, D. K. Atwood, J. Arthur, and M. A. Horne, Search for a Nonlinear Variant of the Schrödinger Equation by Neutron Interferometry, Phys. Rev. Lett. **44**, 765 (1980).

[19] R. Gähler, A. G. Klein, and A. Zeilinger, Neutron optical tests of nonlinear wave mechanics, Phys. Rev. A **23**, 1611 (1981).

[20] J. J. Bollinger, D. J. Heinzen, W. M. Itano, S. L. Gilbert, and D. J. Wineland, Test of the Linearity of Quantum Mechanics by rf Spectroscopy of the $^9Be^+$ Ground State, Phys. Rev. Lett. **63**, 1031 (1989).

[21] T. E. Chupp and R. J. Hoare, Coherence in Freely Precess-ing ^{21}Ne and a Test of Linearity of Quantum Mechanics, Phys. Rev. Lett. **64**, 2261 (1990).

[22] R. L. Walsworth, I. F. Silvera, E. M. Mattison, and R. F. C. Vessot, Test of the Linearity of Quantum Mechanics in an Atomic System with a Hydrogen Maser, Phys. Rev. Lett. **64**, 2599 (1990).

[23] P. K. Majumder, B. J. Venema, S. K. Lamoreaux, B. R. Heckel, and E. N. Fortson, Test of the Linearity of Quantum Mechanics in Optically Pumped ^{201}Hg, Phys. Rev. Lett. **65**, 2931 (1990).

[24] A. Vinante, R. Mezzena, P. Falferi, M. Carlesso, and A. Bassi, Improved Noninterferometric Test of Collapse Models Using Ultracold Cantilevers, Phys. Rev. Lett. **119**, 110401 (2017).

[25] C. K. Hong, Z. Y. Ou, and L. Mandel, Measurement of Subpicosecond Time Intervals Between Two Photons by Interference, Phys. Rev. Lett. **59**, 2044 (1987).

[26] R. J. Glauber, The quantum theory of optical coherence, Phys. Rev. **130**, 2529 (1963).

[27] J.-W. Pan, Z.-B. Chen, C.-Y. Lu, H. Weinfurter, A. Zeilinger, and M. Żukowski, Multiphoton entanglement and interferometry, Rev. Mod. Phys. **84**, 777 (2012).

[28] M. C. Tichy, Interference of identical particles from entan-glement to boson-sampling, J. Phys. B At. Mol. Opt. Phys. **47**, 103001 (2014).

[29] S. Agne, T. Kauten, J. Jin, E. Meyer-Scott, J. Z. Salvail, D. R. Hamel, K. J. Resch, G. Weihs, and T. Jennewein, Observation of Genuine Three-Photon Interference, Phys. Rev. Lett. **118**, 153602 (2017).

[30] A. J. Menssen, A. E. Jones, B. J. Metcalf, M. C. Tichy, S. Barz, W. S. Kolthammer, and I. A. Walmsley, Distinguish-ability and Many-Particle Interference, Phys. Rev. Lett. **118**, 153603 (2017).

[31] V. Giovannetti, S. Lloyd, and L. Maccone, Advances in quantum metrology, Nat. Photonics **5**, 222 (2011).

[32] Z.-E. Su, Y. Li, P. P. Rohde, H.-L. Huang, X.-L. Wang, L. Li, N.-L. Liu, J. P. Dowling, C.-Y. Lu, and J.-W. Pan, Multiphoton Interference in Quantum Fourier Transform Circuits and Applications to Quantum Metrology, Phys. Rev. Lett. **119**, 080502 (2017).

[33] R. Hanbury Brown and R. Q. Twiss, A test of a new type of stellar interferometer on Sirius, Nature (London) **178**, 1046 (1956).

[34] C. Thiel, T. Bastin, J. Martin, E. Solano, J. von Zanthier, and G. S. Agarwal, Quantum Imaging with Incoherent Photons, Phys. Rev. Lett. **99**, 133603 (2007).

[35] R. Schneider *et al.*, Quantum imaging with incoherently scattered light from a free-electron laser, Nat. Phys. **14**, 126 (2018).

[36] S. Aaronson and A. Arkhipov, The computational complexity of linear optics, in *Proceedings of the 43rd Annual ACM Symposium on Theory of Computing, STOC '11* (ACM, New York, NY, USA, 2011), pp. 333–342.

[37] H. Wang, J. Qin, X. Ding, M.-C. Chen, S. Chen, X. You, Y.-M. He, X. Jiang, L. You, Z. Wang, C. Schneider, J. J. Renema, S. Höfling, C.-Y. Lu, and J.-W. Pan, Boson Sampling with 20 Input Photons and a 60-Mode Interferometer in a 10^{14}-Dimensional Hilbert Space, Phys. Rev. Lett. **123**, 250503 (2019).

[38] M.-O. Pleinert, J. von Zanthier, and E. Lutz, Many-particle interference to test Born's rule, Phys. Rev. Research **2**, 012051(R) (2020).

[39] See Supplemental Material at http://link.aps.org/supplemental/10.1103/PhysRevLett.126.190401 for additional details regarding the experimental setup.

[40] H. Yabuki, Feynman path integrals in the Young double-slit experiment, Int. J. Theor. Phys. **25**, 159 (1986).

[41] R. Sawant, J. Samuel, A. Sinha, S. Sinha, and U. Sinha, Nonclassical Paths in Quantum Interference Experiments, Phys. Rev. Lett. **113**, 120406 (2014).

[42] O. S. Magaña-Loaiza, I. De Leon, M. Mirhosseini, R. Fickler, A. Safari, U. Mick, B. McIntyre, P. Banzer, B. Rodenburg, G. Leuchs, and R. W. Boyd, Exotic looped trajectories of photons in three-slit interference, Nat. Commun. **7**, 13987 (2016).

[43] Since the SPADs are not number-resolving, multiphoton events at a single SPAD cannot be excluded. However, such events have a negligible effect on our results in the parameter regime of the experiment [39].

[44] The two-particle Hong-Ou-Mandel experiment corresponds to second-order interference since it only involves two input modes [25].

[45] Second- and third-order terms are a little smaller than expected, which suggests a slight off-center measurement.

[46] Because of a difficult alignment, this result has been obtained with 100 remeasurements of only the configuration *ABCD* and its subconfigurations.

[47] R. Keil, T. Kaufmann, T. Kauten, S. Gstir, C. Dittel, R. Heilmann, A. Szameit, and G. Weihs, Hybrid waveguide-bulk multi-path interferometer with switchable amplitude and phase, APL Photonics **1**, 081302 (2016).

[48] The sensitivity quantifies the smallest change that can be detected in a measurement and depends on the measurement method. On the other hand, the precision is related to the measurement errors of the experimental setup.

[49] S. Oppel, R. Wiegner, G. S. Agarwal, and J. von Zanthier, Directional Superradiant Emission from Statistically Independent Incoherent Nonclassical and Classical Sources, Phys. Rev. Lett. **113**, 263606 (2014).

[50] M. Sabuncu, L. Mišta, J. Fiurášek, R. Filip, G. Leuchs, and U. L. Andersen, Nonunity gain minimal-disturbance measurement, Phys. Rev. A **76**, 032309 (2007).

[51] M. Lassen, M. Sabuncu, A. Huck, J. Niset, G. Leuchs, N. J. Cerf, and U. L. Andersen, Quantum optical coherence can survive photon losses using a continuous-variable quantum erasure-correcting code, Nat. Photonics **4**, 700 (2010).

[52] M. Lassen, L. S. Madsen, M. Sabuncu, R. Filip, and U. L. Andersen, Experimental demonstration of squeezed-state quantum averaging, Phys. Rev. A **82**, 021801(R) (2010).